Monte Carlo Diffusion Model of Polymer Coagulation

Yves Termonia

Central Research and Development, Experimental Station, E.I. du Pont de Nemours, Inc., Wilmington, Delaware 19880-0356

(Received 7 January 1994)

Polymer coagulation is simulated on a lattice by a Monte Carlo diffusion process in which particles move according to the change in local energy. Our model allows, for the first time, a description of the coagulation process beyond the initial quench state and a reproduction of the wide variety of polymer structures that can be obtained, ranging from dustlike to fingerlike to spongelike morphologies. We show that these morphologies are fully controlled by the coagulation rate which itself depends on the miscibility between solvent and coagulant.

PACS numbers: 61.41.+e, 61.20.Ja

Polymer coagulation defines the process by which a polymer solution is quenched in an aqueous nonsolvent, leading to solvent-coagulant exchange and polymer precipitation. That process constitutes the most important step in the formation of polymeric materials through the solution processing route. It is therefore at the basis of a wide range of polymer processes including wet spinning [1], fibridation [2], and membrane formation [3].

In spite of its importance, the kinetics of polymer coagulation is not well understood. Previous work has been restricted to the very early stages of coagulation, *before the onset of phase separation.* These studies were aimed at deriving analytical equations for the mass transfer paths in the thermodynamic equilibrium phase diagram [4], premising that the location of those paths with respect to the liquid miscibility gap controls the ultimate polymer structure. For simplicity, it was also assumed that (i) the diffusion process is purely one dimensional, (ii) thermodynamic equilibrium is always preserved at the coagulant-polymer interface, and (iii) phase separation occurs through nucleation and growth; i.e., the rate of solvent/coagulant exchange is infinitesimally slow.

In view of the great difficulties associated with analytical attempts to describe the development of polymer structure during coagulation, we resort, in the present Letter, to an actual computer simulation of the ternary diffusion process. For simplicity, our approach is limited to a two-dimensional geometry similar to that encountered in typical experimental studies in which a drop of polymer solution is placed between two microscope slides and the coagulant introduced near the edge [5–7]. Our two-dimensional model of diffusion is schematically depicted by the lattice of Fig. 1(a), in which the bottom five rows of sites are occupied by coagulant particles. Coagulant, solvent, and polymer particles will be referred to by indexes 1, 2, and 3, respectively. For simplicity, we assume that the coagulation bath is infinite and well stirred [4], so that solvent particles diffusing into that layer are continuously being removed from the lattice and replaced by coagulant particles. The coagulation process is simulated as follows. We start by picking, at random, a pair of particles—i and j—on nearest neighbor lattice sites. Denoting by α the shell of nearest neighbor particles for that pair [Fig. 1(b)], the rate for an exchange $ij \rightarrow ji$ within α is calculated from [8]

$$\upsilon_{ij\rightarrow ji,\alpha} = \tau_{i,j}^{-1} \exp[\beta(E_{ij,\alpha} - E_{ji,\alpha})/2] , \quad (1)$$

in which $\tau_{i,j}^{-1}$ is related to the mutual diffusion co-

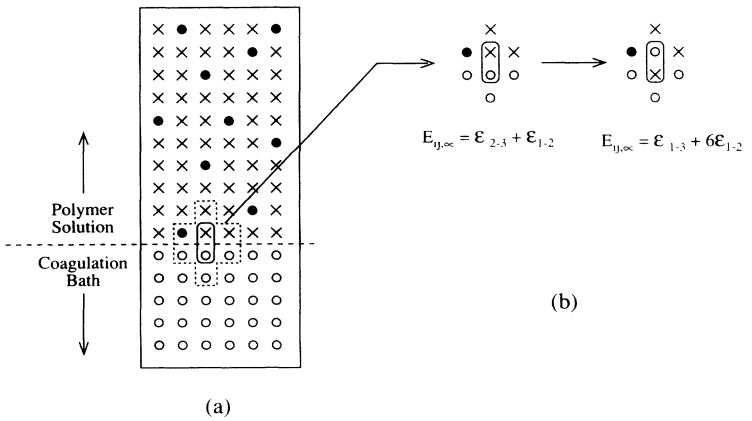

FIG. 1. Schematic representation of our lattice model for polymer coagulation. The polymer, the solvent, and the coagulant particles are denoted by symbols ●, ×, and ○, respectively. The diffusion process is simulated through a series of two-particle exchanges on nearest neighbor lattice sites (a). The rates of exchange are obtained from Eq. (1) in which $E_{ij,\alpha}$ and $E_{ji,\alpha}$ are the interaction energies of the pair with nearest neighbor particles, before and after the exchange; see (b).

0031-9007/94/72(23)/3678(4)$06.00

efficient, $D_{i,j}^{\infty}$, of i and j particles at infinite dilution through [8]

$$D_{i,j}^{\infty} = \tau_{i,j}^{-1}(\delta x)^2 , \quad (2)$$

where δx denotes the unit lattice length. In Eq. (1), all the effects of particle interactions are relegated to the Boltzmann exponent of (half) the energy difference between initial and final states for the pair. That functional form for the dependence of rate on local energy change is guided by the requirement of commutativity of the individual two-particle exchanges [8]. Using Eq. (1) a probability for the exchange is obtained through

$$p_{ij\rightarrow ji,a} = v_{ij\rightarrow ji,a}/v_{\max} , \quad (3)$$

in which $v_{\max}$ denotes the highest rate of exchange among all the pairs on the lattice. A random number is then generated and the exchange is allowed if that number falls below p. After each visit of a pair, the overall "time" t is incremented by $1/v_{\max}n$ in which n denotes the total number of pairs on the lattice [9]. As the coagulant diffuses into the polymer solution, individual polymer particles phase separate into small clusters which also are mobile and aggregate into larger clusters. In our process, small clusters move through a series of one-lattice-unit displacements of entire rows or columns of polymer particles. The rate of displacement of a row or a column is assumed to be the same as that for a single particle, Eq. (1), except for the presence of a prefactor which is chosen inversely proportional to the total number of particles involved in the displacement [10]. Admittedly, other choices for that prefactor are possible. Our model results, however, reveal that details of the cluster diffusion process are of lesser importance than the choice of values for the pair interaction energies ε.

We now turn to an application of the model described above to the coagulation of Nomex, an aromatic polyamide commercialized by DuPont. The polymer dissolves in N-methylpyrrolidone (NMP) and is commonly precipitated in water. Approximate values of the three pair interaction energies $\varepsilon_{1\text{-}2}$, $\varepsilon_{1\text{-}3}$, and $\varepsilon_{2\text{-}3}$ for the system water(1)/NMP(2)/Nomex(3) can be obtained as follows. Graduate cooling of a 50/50 solution of NMP in water shows an onset of phase separation at 7 °C [11]. Fitting that value by the critical solution temperature predicted in Ref. [8] for a binary mixture leads to $\varepsilon_{1\text{-}2} = 0.274kT$ at room temperature and for a coordination number $\kappa = 8$. In the absence of any binary mixture data for the pairs water(1)/Nomex(3) and NMP(2)/Nomex(3), we set $\varepsilon_{2\text{-}3} = 0$ and elect to determine $\varepsilon_{1\text{-}3}$ from the ternary equilibrium phase diagram. An algorithm for estimating the spinodal curve for a given set of $\varepsilon_{1\text{-}2}$, $\varepsilon_{1\text{-}3}$, and $\varepsilon_{2\text{-}3}$ values has been presented in Ref. [12]. A curve fitting of the calculated spinodal to the actual binodal [13] taken from Ref. [6] leads to $\varepsilon_{1\text{-}3} = 1kT$ for $\kappa = 8$. Since the present model study is for a square lattice with $\kappa = 4$, the ε values need to be suitably normalized. To this end, we note that the critical values for phase separation in body-centered cubic ($\kappa = 8$) and square ($\kappa = 4$) lattices are $\varepsilon_{\kappa=8}^{\text{crit}} = 0.31$ and $\varepsilon_{\kappa=4}^{\text{crit}} = 0.88$, respectively [14]. Thus, in our model simulations on the square lattice, we set $\varepsilon_{1\text{-}2} = 0.77$, $\varepsilon_{2\text{-}3} = 0$, and $\varepsilon_{1\text{-}3} = 2.8$ for the system water(1)/NMP(2)/Nomex(3).

We now turn to an estimation of the kinetic parameters $\tau_{i,j}$; see Eq. (1). It is well accepted from experiments on membrane formation [15–17] that a polymer in solution does not consist of individual molecules but, rather, of macromolecular aggregates 20 nm in diameter [15–17]. That aggregation is believed to be caused both by the high polymer concentrations and by the weak solvent power typically used in most coagulation processes. Thus, in our model of elementary particle exchanges on a lattice, we set the unit lattice length $\delta x = 20$ nm. Since the mutual diffusion coefficient of liquids is of the order of 10^{-5} cm^2/sec, use of Eq. (2) leads to $\tau_{1,2} = 4\times 10^{-7}$ sec. The zero-concentration diffusion coefficient of most polymers in good solvents lies in the range 10^{-7}–10^{-6} cm^2/sec [18]. Taking $D^{\infty} = 10^{-6.5}$ cm^2/sec leads to $\tau_{1,3} = \tau_{2,3} = 1.3\times 10^{-5}$ sec. As in Ref. [8], we assume a constancy of the two time constants $\tau_{1,3}$ and $\tau_{2,3}$ and relegate all concentration dependence of the diffusion process to the Boltzmann factors of the local interaction energies; see Eq. (1).

Figure 2(b) shows our model prediction of the coagulated Nomex structure at time $t = 0.02$ sec. The initial concentration of polymer in the solvent equals 20%. The figure clearly reveals the presence of a polymer skin behind which the water diffuses into a series of fingerlike structures, in perfect agreement with experimental observation [6,7]. Since our unit lattice spacing is of the order of 20 nm, the skin thickness is estimated to be in the range 0.2–0.3 μm which again conforms with experimen-

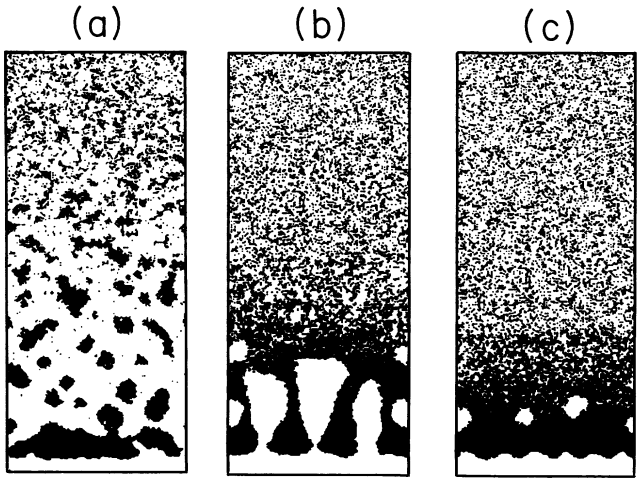

FIG. 2. Effect of the solvent/coagulant miscibility on polymer structure. (a) $\varepsilon_{1\text{-}2} = 0$, (b) $\varepsilon_{1\text{-}2} = 0.77$, and (c) $\varepsilon_{1\text{-}2} = 1.5$. The structures are for a coagulation time $t = 0.02$ sec, except (c) which is for $t = 0.03$ sec. The initial polymer concentration is set at 20%.

tal values [19,20]. The molecular origin of the coagulated finger structure has been the matter of some debate. The prevailing explanation [7] is based on mechanical rupture of the skin which allows the coagulant to burst into fast growing fingers extending deep inside the polymer solution. That mechanism, however, fails to explain the strikingly regular shape and spacing of the fingers observed experimentally [6,7] and correctly reproduced by our approach. Inspection of our model results leads to the following insight. Upon immersion of the polymer solution in the coagulation bath, the fast solvent-coagulant exchange across the interface, combined with the large repulsive forces between Nomex and water particles ($\varepsilon_{1\text{-}3}=2.8kT$), causes an immediate precipitation of the polymer at the interface. That process is too fast for any segregation of the polymer into polymer-rich and polymer-poor domains to occur and a thin skin rapidly forms. Since the polymer concentration is rather low, that early skin does not have a uniform thickness and defects are present along its contour. These defects then form the initiation pores for coagulant penetration into fast growing fingers. In support of our proposed mechanism for finger formation, we note that fingers are never observed when a skin is absent or when the polymer volume fraction is too high, i.e., when skin defects are less probable. Finally, it is also worth noting that the coagulated finger structures of Fig. 2(b) bear a close resemblance to the viscous fingering instabilities obtained when a fluid of lower viscosity is injected into a more viscous one [21].

Actual coagulation experiments [4,7] have also revealed that the miscibility of the solvent and coagulant is one of the most important factors determining the morphology of the precipitated polymer. Figures 2(a) and 2(c) show the polymer structures predicted by our model in the limits of very good ($\varepsilon_{1\text{-}2}=0$) and quite poor ($\varepsilon_{1\text{-}2}=1.5$) miscibilities of solvent and coagulant. All the structures are for approximately the same time $t=0.2$–0.3 sec. In the case of good miscibility [$\varepsilon_{1\text{-}2}=0$, Fig. 2(a)], the polymer is seen to coagulate into large agglomerates of ca. 0.3 μm in diameter, leading to a "dust-like" structure. Although the agreement may be fortuitous, it is interesting to note that the latter value is close to our estimation of the skin thickness and also to the diameter of the secondary particles observed during coagulation of cellulose-acetate membranes [16]. For very immiscible solvent and coagulant [$\varepsilon_{1\text{-}2}=1.5$, Fig. 2(c)], a very dense polymer structure is obtained in which the coagulant forms spherical pores (spongelike structure) behind a thick skin. It is interesting to note that the sequence of morphologies obtained in Fig. 2 through a decrease in solvent/coagulant miscibility is also very similar to that obtained experimentally [7] through an increase in the initial polymer concentration. This is easily understandable since a decrease in solvent/coagulant miscibility effectively makes solvent and polymer particles more alike as far as the coagulant is concerned.

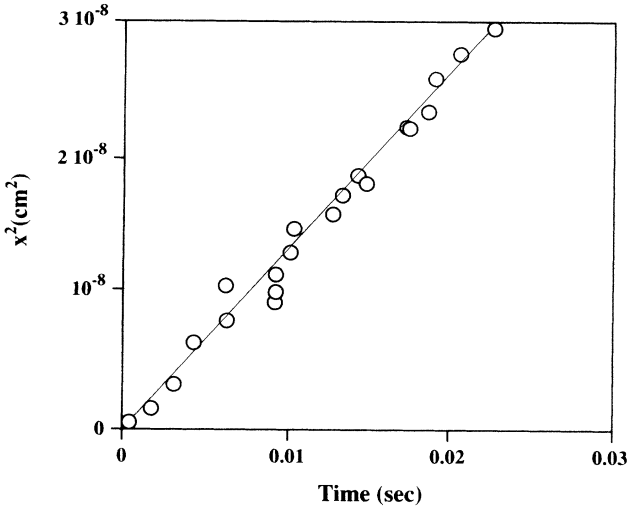

FIG. 3. Time dependence of the penetration depth (squared) of the fingers studied in Fig. 2(b).

Figure 3 shows the time dependence of the depth of penetration of the fingers of Fig. 2(b). The figure clearly shows that, when distances are squared, the dependence is linear at all times, as observed experimentally [7,19]. Our calculated diffusion coefficient $D=1.3\times10^{-6}$ cm^2/sec is in full agreement with the ca. 1.6×10^{-6} cm^2/sec estimate that can be obtained from actual photomicrographs (Fig. 7 of Ref. [6]). A study of the penetration depth of the coagulation fronts for Figs. 2(a) and 2(c) leads to diffusion coefficients of 10^{-5} and 2×10^{-7} cm^2/sec, respectively. Our results thus definitely show that the morphologies of Figs. 2(a)–2(c) are fully controlled by the coagulation rate, as has been widely anticipated in the literature.

Because of CPU limitations, our results are for short coagulation times ($t<0.03$ sec) which has allowed the study of structures no larger than a few microns in depth. It could be argued that the results of the present work are therefore not representative of the fully coagulated structures that sometimes require up to a few minutes to obtain. In support of our results, however, we recall that Fig. 3 clearly indicates that the diffusion coefficient of the coagulation front is time independent. Since the value of that coefficient fully dictates the structure of the coagulated polymer, a change in morphology at later times remains improbable and the gross morphology of the final polymer structure should be adequately described by our model results.

I wish to thank Dr. Greg Dee for helpful discussions and for a critical reading of the manuscript.

[1] W. E. Dorogy and A. K. St. Clair, J. Appl. Polym. Sci. **43**, 501 (1991).

[2] G. C. Gross, DuPont Progress Report, HT 68-7, 1968 (unpublished).

[3] R. E. Kesting, *Synthetic Polymeric Membranes* (Wiley, New York, 1985), 2nd ed.
[4] J. E. Anderson and R. Ullman, J. Appl. Phys. **44**, 4303 (1973); C. Cohen, G. B. Tanny, and S. Prager, J. Polym. Sci.: Polym. Phys. Ed. **17**, 477 (1979); A. J. Reuvens, J. W. A. van den Berg, and C. A. Smolders, J. Membr. Sci. **34**, 45 (1987); A. J. Reuvers and C. A. Smolders, J. Membr. Sci. **34**, 67 (1987); A. J. McHugh and L. Yilmaz, J. Membr. Sci. **43**, 319 (1989); C. S. Tsay and A. J. McHugh, J. Polym. Sci.: Polym. Phys. Ed. **28**, 1327 (1990).
[5] M. A. Frommer and D. Lancet, in *Reverse Osmosis Membrane Research*, edited by H. K. Lonsdale and H. E. Podall (Plenum, New York, 1972), p. 85.
[6] H. Strathmann, in *Materials Science of Synthetic Membranes*, ACS Symposium Series No. 269 (American Chemical Society, Washington, DC, 1985), p. 165.
[7] H. Strahmann, K. Kock, P. Amar, and R. W. Baker, Desalination **16**, 179 (1975).
[8] Z. Alexandrowicz and Y. Termonia, Mol. Phys. **38**, 47 (1979).
[9] Y. Termonia, P. Meakin, and P. Smith, Macromolecules **18**, 2246 (1985).
[10] P. Meakin, Phys. Rev. Lett. **51**, 1119 (1983).
[11] Y. Termonia (unpublished).
[12] Y. Termonia, Mol. Phys. **38**, 65 (1979).
[13] The error involved in fitting the theoretical spinodal curve to the experimental binodal line is not expected to be of importance since, in the highly immiscible systems under study, binodal and spinodal curves are close to each other.
[14] C. Domb, Adv. Phys. **9**, 149 (1960).
[15] R. E. Kesting, J. Appl. Polym. Sci. **41**, 2739 (1990).
[16] K. Kamide and S. Manabe, in *Materials Science of Synthetic Membranes* (Ref. [6]), p. 197.
[17] M. Panar, H. H. Hoehn, and R. R. Hebert, Macromolecules **6**, 777 (1973).
[18] *Polymer Handbook*, edited by J. Brandrup and E. H. Immergut (Wiley, New York, 1975), 2nd ed.
[19] R. L. Riley, J. O. Gardner, and U. Merten, Desalination **1**, 30 (1966).
[20] H. K. Lonsdale, U. Merten, and R. L. Riley, J. Appl. Polym. Sci. **9**, 1341 (1965).
[21] J. Nittmann, G. Daccord, and H. E. Stanley, Nature (London) **314**, 141 (1985); J. Nittmann and H. E. Stanley, Nature (London) **321**, 663 (1986); D. Benisimon, L. P. Kadanoff, S. Liang, B. I. Shraiman, and C. Tang, Rev. Mod. Phys. **58**, 977 (1986); E. Ben-Jacob and P. Garik, Nature (London) **343**, 523 (1990); K. R. Bhaskar, P. Garik, B. S. Turner, J. D. Bradley, R. Bansil, H. E. Stanley, and J. T. LaMont, Nature (London) **360**, 458 (1992).

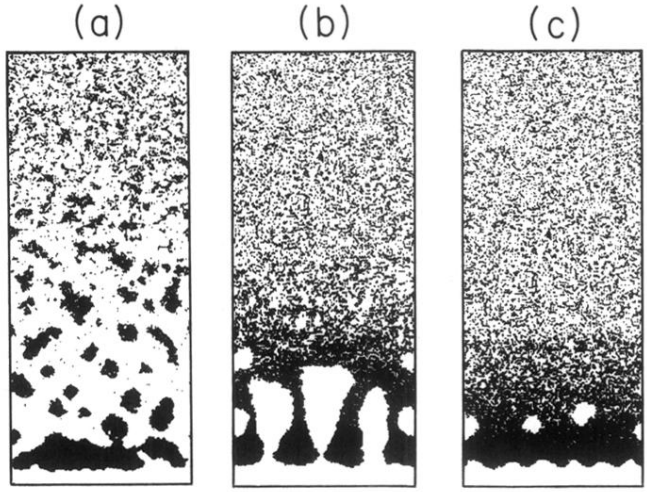

FIG. 2. Effect of the solvent/coagulant miscibility on polymer structure. (a) $\varepsilon_{1\text{-}2}=0$, (b) $\varepsilon_{1\text{-}2}=0.77$, and (c) $\varepsilon_{1\text{-}2}=1.5$. The structures are for a coagulation time $t=0.02$ sec, except (c) which is for $t=0.03$ sec. The initial polymer concentration is set at 20%.